

# A novel capsule-based smell test fabricated via coaxial dripping

A. Said Ismail<sup>a</sup>, Gregory R. Goodwin<sup>b</sup>, J. Rafael Castrejon-Pita<sup>a</sup>, Alastair J. Noyce<sup>b</sup> and Helena S. Azevedo<sup>a</sup>

<sup>a</sup> School of Engineering and Materials Science, Queen Mary University of London, London E1 4NS, United Kingdom

<sup>b</sup> Preventive Neurology Unit, Wolfson Institute of Preventive Medicine, Barts and the London School of Medicine and Dentistry, Queen Mary University of London

## Abstract

In this paper we demonstrate that aromatic oil capsules, produced by dripping droplets, can offer a simple, yet effective, testing tool to aid in the diagnosis of various diseases, in which the loss of smell is a key symptom. These include chronic neurological conditions such as Parkinson's and Alzheimer's disease, and acute respiratory infections such as that caused by Covid-19. The capsules were fabricated by concentrically dripping oil/alginate droplets, from a coaxial nozzle, into an oppositely charged ionic liquid. This fabrication technique enables full control over the capsule size, the shell thickness, and the volume of the encapsulated oil. After formation, liquid capsules were left to dry and form a solid crust surrounding the oil. The prototype test consists of placing a standardized number of capsules between adhesive strips that users crush and pull apart to release the smell. In addition to the fabrication method, a simple mathematical model was developed to predict the volume of encapsulated oil within the capsule in terms of the flow rate ratio and the nozzle size. Tensile tests show that capsule strength is inversely proportional to its size owing to an increase in the shell thickness. By increasing the alginate concentration, the load required to rupture the capsule increases, to the point where capsules are too stiff to be broken by a fingertip grip. Results from a preliminary screening test, within a group of patients with Parkinson's disease, found that smells were detectable using a 'forced choice' paradigm.

**Keywords:** encapsulation; drop dripping; ionic gelation; olfaction; smell test

## 2. INTRODUCTION

Although often overlooked, olfaction – the sense of smell – significantly aids our interaction with the environment. Its absence is associated with isolation, anhedonia [1], and depression [2]. The sense of taste is heavily reliant on a functioning olfactory system [3] and a reduction (hyposmia) or loss (anosmia) of olfaction may be a sign of a head trauma, the result of ageing or an acute or chronic medical disorders [4]. Loss of smell is recognized to be an early feature of neurodegenerative conditions, such as Alzheimer's and Parkinson's disease, with a prevalence of up to 90% in Parkinson's disease [6]. Early detection of neurodegenerative diseases under the assumption that those at the earliest stages will be more likely to gain benefit from neuroprotective clinical trials and future treatments [7]. Separately, smell loss has emerged as an important feature of COVID-19 infection, with ~65% of those testing positive for COVID-19 experiencing subjective loss of smell or taste, compared to 22% of those testing negative [5]. People who are

negative for COVID could still lose their sense of smell because screening tests for COVID are neither 100% sensitive or specific. Also there are other causes of smell loss such as head injury, viral infection and increasing age.

The most commonly used smell tests are “scratch-and-sniff”, in that they consist of a printed slurry of microencapsulated beads of oil set within an adhesive material. This type of bead encapsulation comes from a polyoxymethylene urea matrix [8], was first produced in 1984 and is now considered the gold standard test to detect anosmia and hyposmia [9, 10]. The most commonly used test, the University of Pennsylvania Smell Identification Test (UPSIT), has 40-item “scratch-and-sniff” and requires users to make a forced choice for each odor based on four options [11]. While effective, scratch-and-sniff tests are expensive. The price of only a single test unit is around \$26.95 [12], making it ill-suited to large screening programs likely to require thousands of tests. Furthermore, the amount of odour released is dependent on the extent to which the individual scratches the “scratch-and-sniff” strip. Based on our experience of using the 40-item UPSIT for large-scale testing, 10-15% of tests were either not returned or well incorrectly completed [13].

Olfactory displays are an alternative method of odour delivery composed of stocked odour material that can be vaporised and released on demand and then smelled by the user [14]. They are an emerging technology in the field of virtual reality [15]. Vapours can be blended to create specific and complex odours and displays such as these can be adjusted and controlled to produce specific quantities, and therefore potencies, of odour. This is advantageous where consistent odour potency is required such as in a screening test. Nevertheless, olfactory displays are expensive and impractical to mass produce for screening and their capability to blend odours is unnecessary when assessing a subject’s ability to smell individual odours. Another approach of odour delivery is the compressed cylinders, however, these are expensive to produce and not practical; giving the possible dangers associated with compressed substances and the difficulty in production and packaging for a large screening study which requires many thousands of tests to be distributed easily.

Here, we propose an alternative smell test consisting of capsules of a calcium alginate hydrogel crust surrounding a droplet of scented oil. The capsule can be ruptured manually, for the oil’s odour to be released. The capsules are formed by co-extrusion dripping from a coaxial double-nozzle, enabling rapid, continuous production. Alginate is safe and frequently used to encapsulate a variety of products (flavors, oils, vitamins, dyes, drugs, cells) in the food, textile, cosmetic and pharmaceutical industries to preserving materials for long time periods [16]. This is possible due to the stability of the alginate matrix, formed by the simple and fast ionic gelation reaction that forms a nontoxic material.

Past works have presented various techniques to fabricate oil-encapsulated alginate capsules with spherical or tubular shape, including microfluidics, jet-cutting, vibrating jet, spray-drying,

coextrusion dripping, dispersion [16, 17]. Some of these techniques have been characterized, such as the coaxial-jetting used to fabricate oil-encapsulated alginate microfibers [17], but others such as coextrusion dripping lack such characterization hindering their capability to produce controlled capsules. To our knowledge, the use of oil-containing alginate capsules has never been previously used to test olfaction.

## 2. MATERIAL AND METHODS

### 2.1. Materials

Alginic acid sodium salt from brown algae (medium viscosity) was obtained from Sigma Life Sciences and calcium chloride anhydrous (BioReagent) from Sigma-Aldrich. Aromatic oils (Cherry, Coconut, Clove, Orange (all Aromatherapy®), Menthol (MysticMoments®) and Onion (EcoAurous®)) were used as capsule core materials. Alginate (polymer) solutions were prepared at 2.0 and 4.0 wt% concentrations by dissolving the polymer in tri-distilled water. The polymer was let to dissolve for at least 8 hours to achieve homogenous solutions. All calcium chloride aqueous solutions were prepared at a 1.0 M concentration. Aromatic oils were used undiluted and all solutions were stored at room temperature (25 C) in PTFE bottles prior used and then transferred into plastic 5.0 ml syringes. A cone/plate viscometer (Brookfield DV-1) was used to measure the viscosity of the alginate solutions and the oil, while a pendent drop technique was adopted to measure the liquid surface tension and the liquid-liquid interfacial tension (Table 1).

Table 1 Properties of the liquids used in the experiments

Liquid	$\rho$ (kg·m <sup>-3</sup> )	$\sigma$ (mN·m <sup>-1</sup> )	$\mu$ (mPa·s)
Alginate 2%/ air	1050	68.5	150
Alginate 4%/ air	1080	46.8	990
Cherry oil/ air	918	20.25	34.8
Cherry oil/Alginate 2%	-----	46.4	-----
Cherry oil/ Alginate 4%	-----	33.4	-----

## 2.2. Experimental method

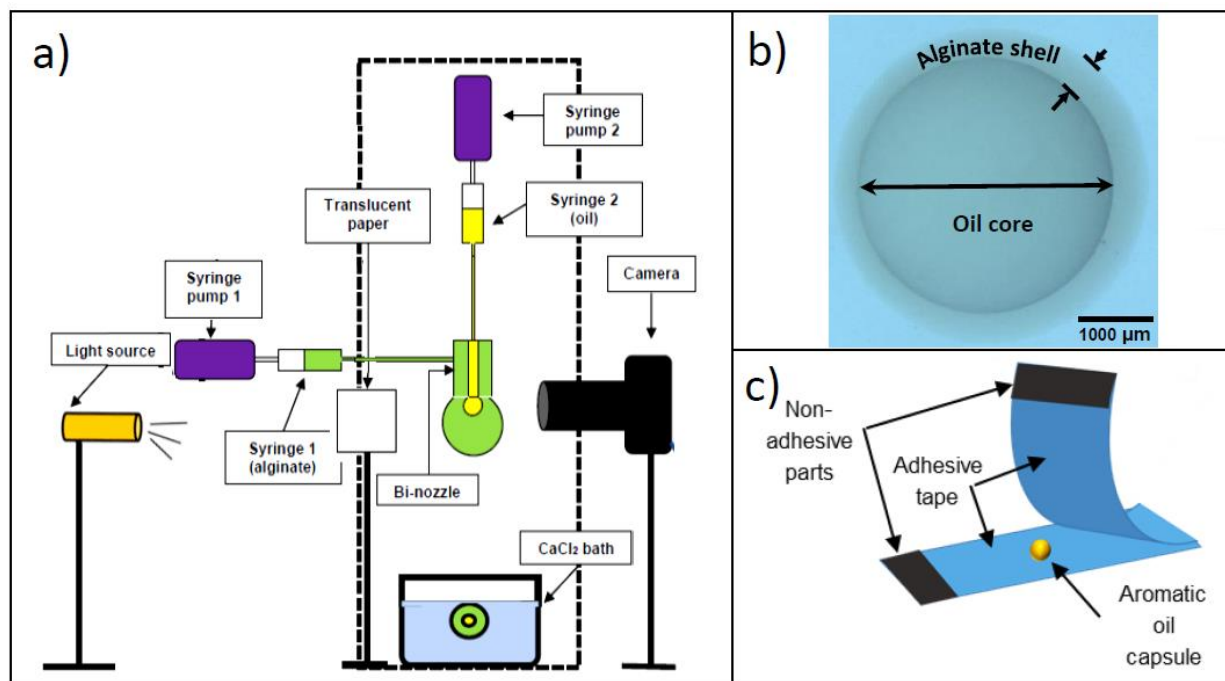


**Figure 1.** a) The experimental set up for the encapsulation process, b) the crosslinked capsule under the microscope showing the alginate shell and the encapsulated oil in the core, and c) the smell test delivery package.

Capsules were fabricated using a coaxial drop dripping system. The apparatus consists of a coaxial nozzle manufactured in-house (Figure 1a) where the inner needle was made from stainless steel with a diameter  $dn_i = 0.9$  mm and a glass needle with outer diameter  $dn_o = 3.0$  mm. This arrangement facilitated the visualization of the coaxial drop formation. The tips of the inner and the outer needles were vertically set at the same height. Capsule formation was visualized by a high-speed camera (Chronos 1.4) and a lamp (Schott KL 1500) directed onto an optical diffuser to provide a uniform background. This camera was used to identify the conditions for successful encapsulation. Two syringe pumps (Harvard Apparatus PHD 2000 HPSI), running simultaneously, fed the coaxial nozzle with the capsule materials. The first syringe pump infused alginate solution from a 50 ml syringe, through plastic tubing, into the outer nozzle. The second syringe pump infused scented oil from a 5.0 ml syringe, via plastic tubing, into the inner needle. The continuous injection of both immiscible liquids led to the formation, and subsequently breakup, of a coaxial drop in which the scent oil was encapsulated inside the alginate solution. The double-nozzle was held vertically at a height of 25.0 mm above the surface of the 1.0 M CaCl<sub>2</sub> solution bath (measured from the nozzle tip). The ionic gelation of alginate was triggered once the droplet touched the calcium solution during the dripping process into the solution bath, where divalent cations form a crosslinked shell of alginate with the scent oil contained inside (Figure 1b).

After 10 min gelation, capsules were removed from the calcium chloride solution using a spatula, and then left to dry for 24 hours on paper filter under ambient conditions (24 °C). Then, the capsules were placed in a transparent petri dish for characterization. The size and thickness of the capsules were recorded by optical microscopy (using a Olympus SZX16 microscope) before and after drying. Finally, tensile tests were carried out on the dry capsules using a compression-testing machine (Instron 3342, 5 and 50 N load cell) to examine the load required to break the capsules.

### 3 RESULTS AND DISSCUSION

#### 3.1 Encapsulation process

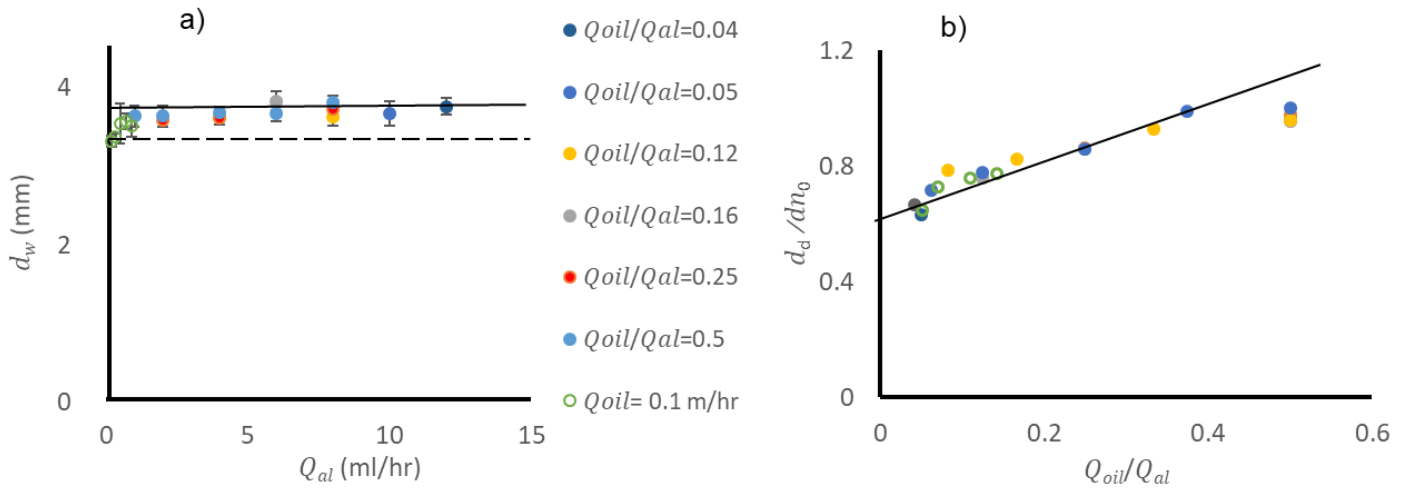
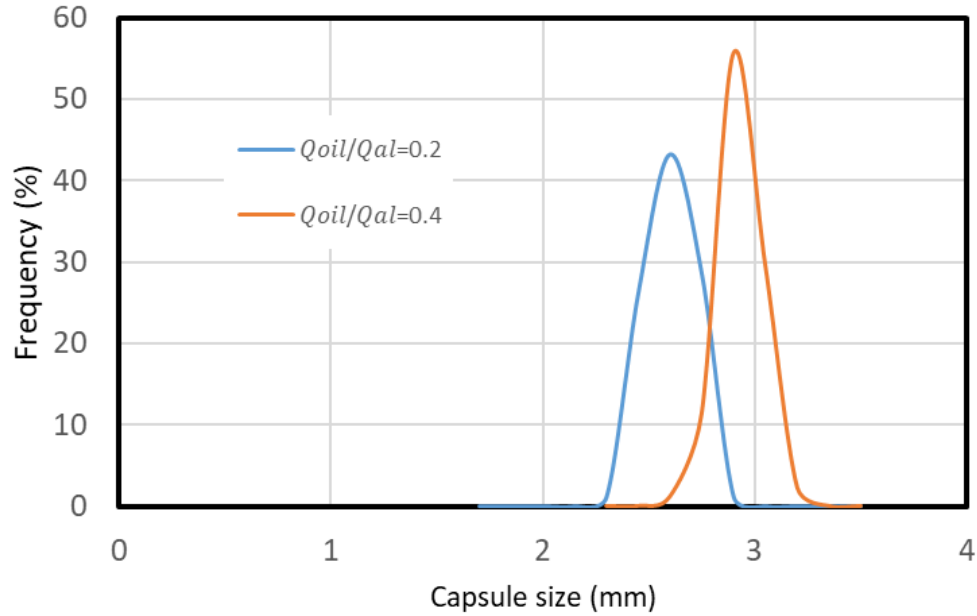


**Figure 2.** Size of measured (a) wet capsules diameter  $d_w$ , and (b) dry capsules diameter  $d_d$  for different flow rates. Closed symbol refers to 2% alginate capsules, while open symbol is for 4% alginate capsules at.

Coaxial drops (oil drop inside alginate drop) were formed at the tip of the coaxial nozzle as a result of the continuous injection of alginate and oil liquids at constant flowrates  $Q_{al}$  and  $Q_{oil}$ . A coaxial drop detached from the nozzle when its body weight was greater than the capillary force holding it at the rim of the nozzle. This results in a drop with a diameter that follows the scaling  $d_w/dn_0 = 2\alpha B^{-\beta}$ , where  $B = |\rho_i - \rho_o|gdn_0^2/4\sigma$  is Bond number,  $\rho_i$  and  $\rho_o$  are the drop and the surrounding medium densities,  $\sigma$  is the outer liquid surface tension, and  $\alpha$  and  $\beta$  are fitting parameters with values 4.46 and 0.356 respectively [18]. According to this approximation, the liquids flow rate does not have an effect on the detached drop size, but only to the frequency of drop production. Figure 2a shows the detached coaxial drop size in terms of the alginate and oil flow rates demonstrating this argument. As seen, the drop average size for 4% alginate solution (dashed line) is slightly lower than that of the 2% alginate (solid line) given differences in surface tension of the alginate solutions, Table 1.

After the alginate coaxial drop is cross-linked by the calcium chloride and are left to dry, the shell thickness shrinks giving a different dry capsule size. The final capsule size depends on the oil to



alginate flow rate ratio through the relation  $d_d/dn_o = C(Q_{oil}/Q_{al})^k$  (Figure 2b) as evaporation in the alginate shell increases with its thickness.  $C$  and  $k$  are fitting parameters that reflect the contraction of the alginate bead during drying with values 0.2 and 1.2 respectively.

**Figure 3.** Capsules size distribution.

Total of 180 measurement were taken to show the dry capsule size histograms corresponding to two different flow rates fractions,  $Q_{oil}/Q_{al} = 0.2$  and  $0.4$  (Figure 3). In addition, it can be seen that a higher flow rate ratio results in a more uniform size distribution (i.e. the relative standard deviations were found to be 4.7% and 2.7%, respectively). This reflects the high uniformity of the produced capsules.

Experiments were conducted with different alginate and oil flow rates to identify the conditions for optimum encapsulation. The range of flow rates studied were  $Q_{al} = 0.2$  to  $16$  ml/hr and  $Q_{oil} = 0.1$  to  $8$  ml/hr. Figure 4a shows the encapsulation parameters for a 2% alginate solution. As observed, single oil drops are successfully encapsulated inside alginate (circle symbols) for conditions where  $Q_{oil}/Q_{al} < 0.5$ . For higher flow rate ratios, the volume of alginate supplied is not enough to cover the oil drop and the oil escapes and fails to produce the capsule (rectangular symbols). The same flow rate limit was observed for 4% alginate solutions (Figure 4b). However, unlike the encapsulation experiments with 2% alginate, another behavior was found where more than one oil drop could be encapsulated inside the alginate (triangle symbols). This was found to occur at  $Q_{oil} > 0.5$  ml/hr and is explained by the differences in the interfacial tension between oil and the 4% and 2% alginate, Table 1. This difference permits the detachment

of smaller oil drops from the inner nozzle and hence more than one oil drop can drip within the outer drop.

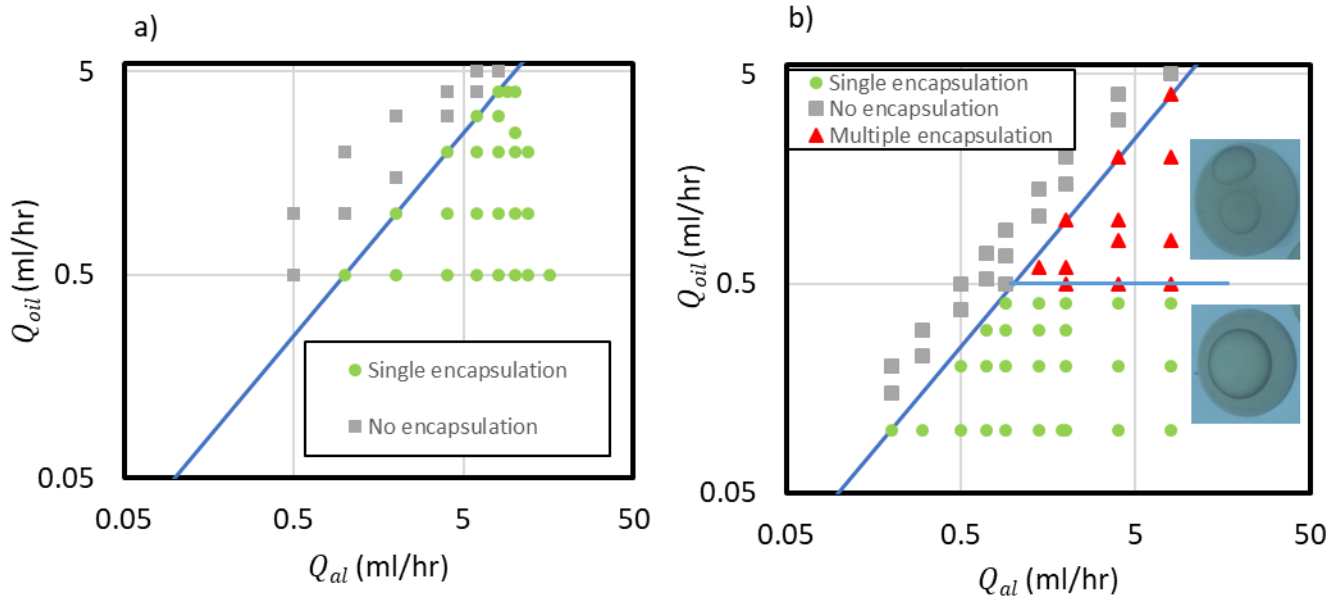


**Figure 4.** Encapsulation map for a) 2% alginate capsules and b) 4% alginate capsules.

The volume of aromatic oil that can be encapsulated, for a coaxial drop formation, is readily obtained from the flowrate of the inner needle  $Q_i = V_{di}/t_b$ , where  $V_{di}$  is the volume of the inner drop and  $t_b$  is the breakup time of the coaxial drop. On the other hand, the outer needle flow rate is given by  $Q_o = V_{do}/t_b$ , where  $V_{do} = V_T - V_{di}$ , and  $V_T$  is the total volume of the coaxial drop just before the breakup. Assuming that  $V_T \sim dn_o^3$ , the outer needle flow rate is then given by  $Q_o \cong (dn_o^3 - V_{di})/t_b$ .

From this analysis a simple relation of the encapsulated drop volume is obtained as

$$V_{di}/dn_o^3 \cong Q_i/Q_T, \quad (1)$$

where  $Q_T = Q_i + Q_o$ . Our experimental data shows an excellent agreement with this relationship (see Figure 5).

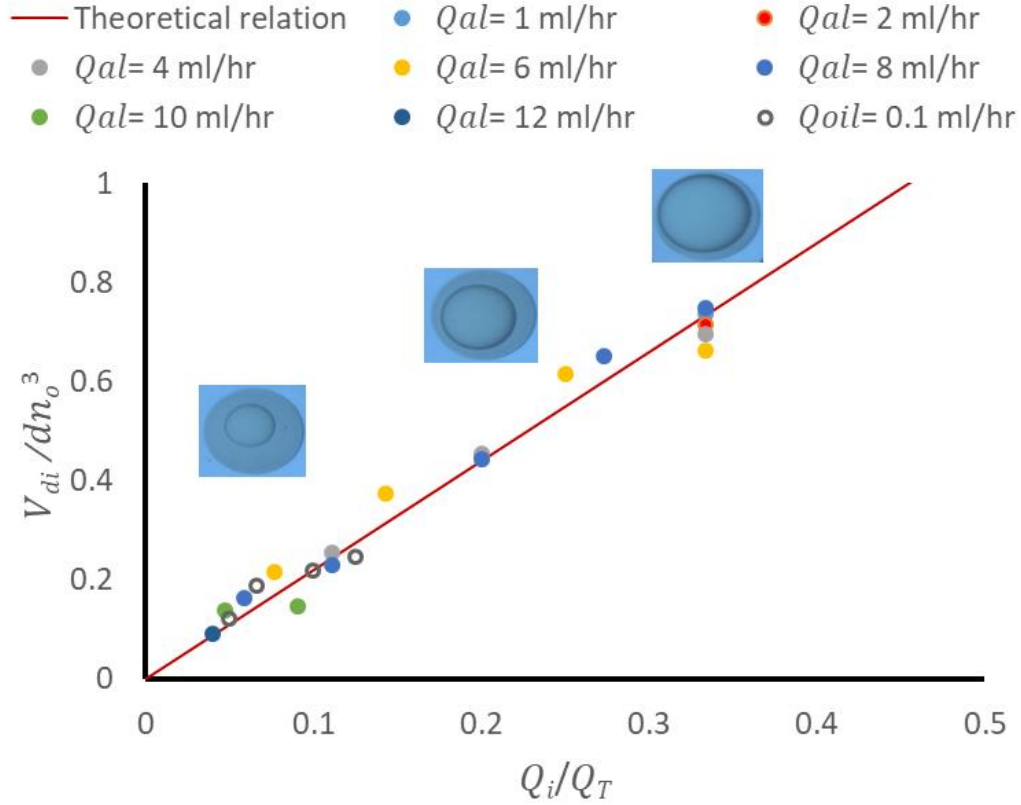


**Figure 5.** Dimensionless encapsulated volume  $V_{di}/dn_o^3$  as a function of the flow rate ratio  $Q_i/Q_T$ .

### 3.2 Capsule material characterisation

The capsule strength in terms of wall thickness was characterised to identify conditions where they could be ruptured by a fingertip grip to release the odour. Capsules of 2.0% and 4.0% alginate concentrations were tested and the maximum load required to break them was measured using the compression to failure test. As expected, larger deformations were required to break larger capsules (Figure 6a), and decreasing the capsule size increased the rupture load. The rupture load as a function of the thickness is found in Figure 6b. Small capsules were found to have a thicker shell and required an increased load to rupture. Additionally, our results indicate that the rupture load dramatically increases with alginate concentration as this results in an excess of polymer chains becoming crosslinked within the gel making the shell stiffer. These results are consistent with the behavior observed elsewhere, on the production of oil-core Ca-alginate capsules [19]. Importantly, our test shows that the load required to break all the 2.0% alginate capsules (25 to 45  $\mu\text{m}$  thickness) is below the 6.0 N fingertip critical grip [20] making them ideal for patient use. At



4.0% alginate concentrations, capsule thicknesses higher than 33  $\mu\text{m}$  were found to break above the critical fingertip grip limit, making these capsules inappropriate for patient use.

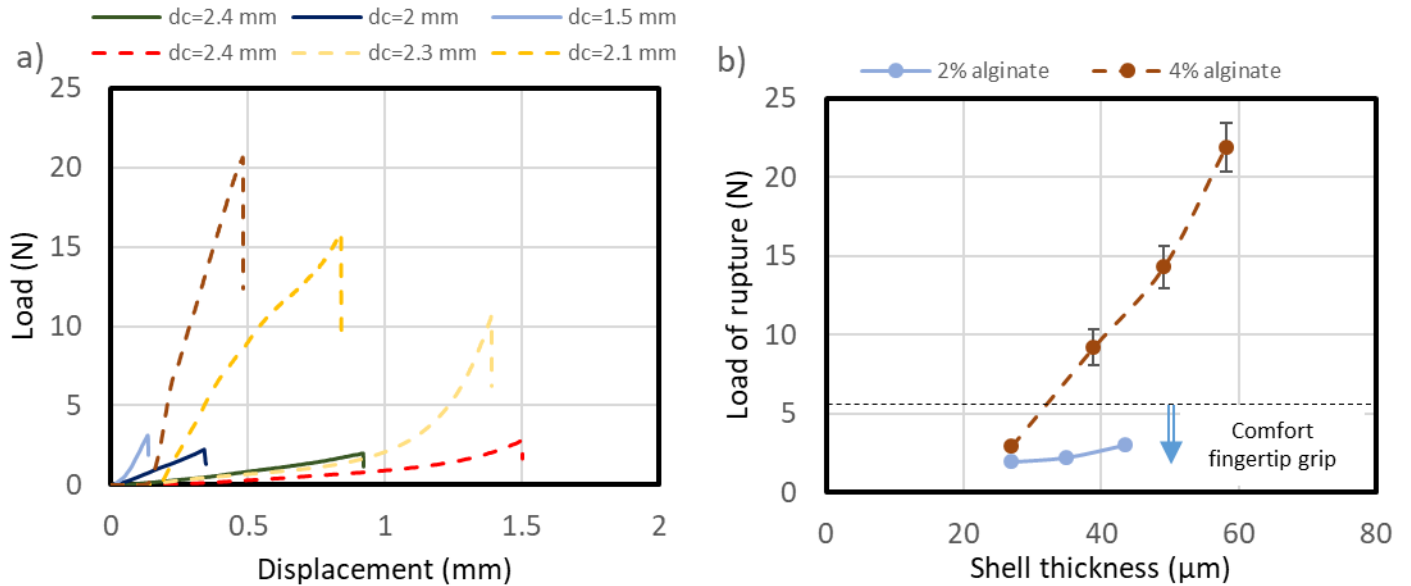


**Figure 6.** Mechanical strength of various capsules. a) Deformation of capsules versus the applied load. b) Shell thickness versus the load required to rupture the capsule.

### 3.3 Smell test performance

Capsules were placed between two strips of single-sided tape where the capsules are crushed between fingers or between the thumb and a solid surface. The tape strips are then peeled apart and the odour is released and can be detected. Sketch of the capsule delivery method is illustrated in Figure 1c and photos of the unit are shown in Figure 7. The unit has dimensions of 7 cm long and 2 cm width. In our tests, 48 of these delivery devices were manufactured, number-coded (associated with a number) and stored in separate plastic bags before testing with patients.

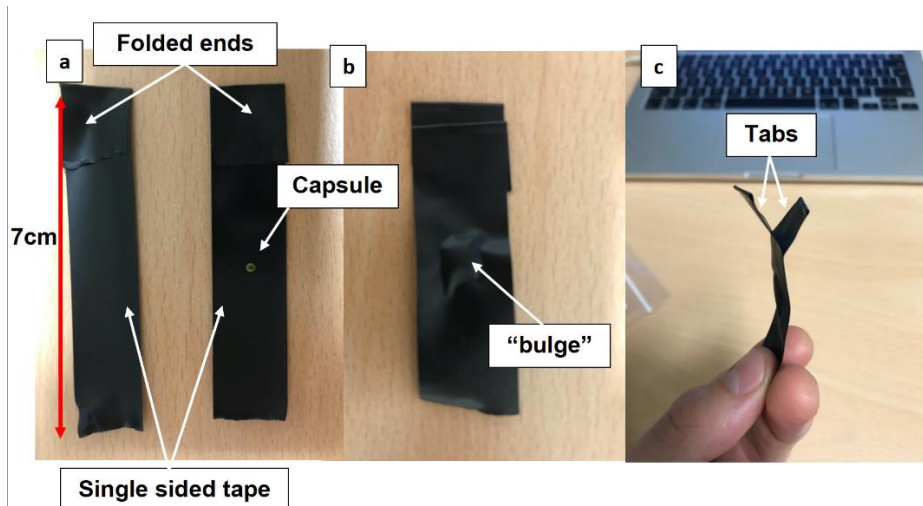


**Figure 7.** Photos of the proposed capsule delivery unit.

A small group of eight patients with Parkinson's disease were recruited to perform two smell battery runs; one “scratch-and-sniff” test (SSA) containing six odours (coconut, menthol, cherry, orange, clove and onion) and the other consisting of the same six odours but using the alginate-encapsulated sniff test (EST). A random number generator determined which test battery would be performed first. The scratch-and-sniff was delivered in the form of a booklet where patients were asked to scratch individual sections to then identify the odour released from a list of four options (one correct option and three distractor options). Odours were different for each run and, once completed. The EST battery consisted of the same six odours and patients had a list of four options – consistent with the scratch-and-sniff test. Each time, after scratching or rupturing an item, the patient was asked to immediately smell and either communicate or circle an answer. There was no time limit, though both types of test usually took around 5 minutes to complete. Patients were given a score out of six for both tests and asked which testing method they preferred to perform of the two, including the reasons for their choice. During the test, all EST capsules (n = 48) were ruptured successfully, releasing the odour. No issues were reported on the manipulation and operation of the EST.

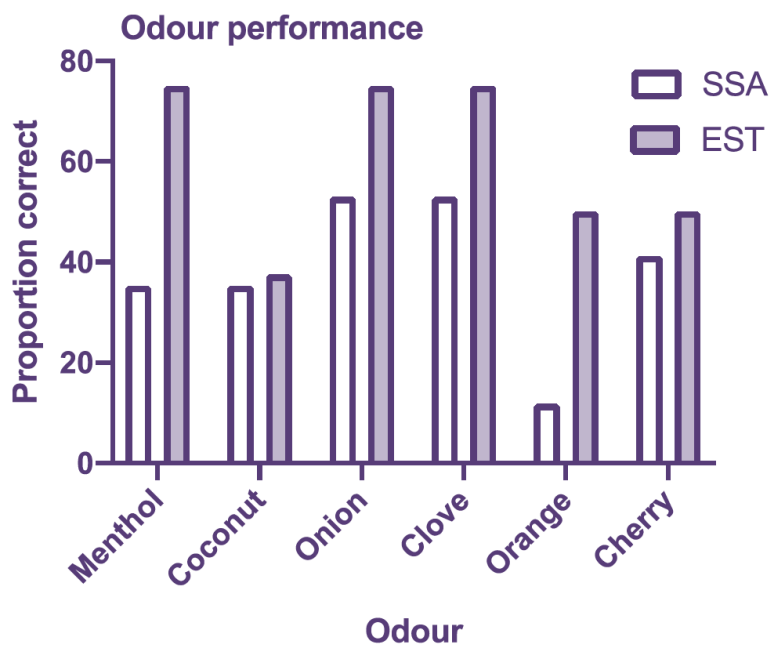


**Figure 8.** Comparison between the performances of our encapsulated smell test (EST) and the scratch and smell test (SSA).

Figure 8 compares the percentage of participants correctly identifying a particular odour for each test. For both tests, onion and clove odours were some of the easiest to identify. As seen, odours were easier to identify in the EST exercise (oil volumes of  $5.0 \text{ mm}^3$  was encapsulated and released while breaking). When asked, five out of the eight participants said they preferred the encapsulated

smell delivery method to the scratch-and-sniff method (primarily citing the relative ease process of rupturing the capsules, particularly for those with tremors, compared to scratching).

#### 4. CONCLUSIONS

In this study, we present a method that uses drops dripping from a coaxial nozzle to fabricate a cheap and fast smell test. The test consists of rupturing alginate capsules containing a scented oil to then identify the released odour. Unlike the traditional “scratch and sniff” testing, the amount of released odor can be controlled more effectively by the encapsulated volume in the proposed single capsule-based approach. The encapsulation process of aromatic oils into alginate was characterized and a parametric map for conditions for the successful encapsulation was established. The proposed method is consistent and produces homogeneous capsules in both size and volume of scented oil. Capsules are stable for long time periods at room temperature and, in a small proof-of-concept study, the capsules effectively and consistently release odour when ruptured by participants showing a better performance in comparison with the traditional scratch and sniff test.

Our findings indicate that aromatic oil is successfully encapsulated for flow rate ratios  $Q_{oil}/Q_{al} < 0.5$ . For low oil/alginate interfacial tensions (33 mN/m), and  $Q_{oil} > 0.5$  ml/hr, we found conditions where more than one oil drop can be encapsulated. A simple mathematical relation,  $V_{ai} \cong \frac{dn_o^3 Q_i}{Q_r}$ , was derived and experimentally verified to determine the volume of oil encapsulated.

This relationship indicates that the amount of encapsulated oil is independent on the properties of the injected liquids and is only a function of the flow rate ratio and the external nozzle size. The mechanical testing of the capsules indicate that 2.0 % alginate capsules are appropriate for patient use as they can be easily ruptured by a fingertip grip, particularly for elderly people who might have developed neurological conditions such as Alzheimer's and Parkinson's diseases. The proposed device may be used also to diagnose COVID-19. Current estimates suggest over 65% of those who have had COVID-19 had a reduced smell sense [5] and assessing smell and taste may predict a positive COVID-19 antigen test better than assessing fever or dry cough.

Our novel encapsulated test advantage over the scratch-and-sniff delivery method is that oil quantity, and therefore odour potency, can be precisely controlled so that an optimum potency, at which sensitivity and specificity of the test is highest, can be established. However, more research is required to quantify this value and it may vary depending on whether a test is screening for COVID-19, neurological conditions or another cause of hyposmia, as the extent of olfactory dysfunction may differ with each condition.

**Ethics.** Patients were tested as part of the East London Parkinson's Disease Project (research ethics reference number 18/SW/0255). Patients were recruited from the Parkinson's Disease Clinic at

The Royal London Hospital over 3 separate clinic days. After their clinic consultation, patients were asked whether they would like to partake in a study assessing sense of smell. Those that agreed completed both a scratch-and-sniff smell test and the novel oil encapsulated smell test.

**Authors' contributions.** A.S.I., H.S.A. and A.J.N. were involved in the design of the study; A.S.I., G.R.G. and J.R.C. performed the experiments; A.S.I. analysed the data and developed the theoretical relations; A.S.I., G.R.G., J.R.C. A.J.N. and H.S.A. were involved in drafting the manuscript.

## REFERENCES

1. Keller A, Malaspina D. 2013 Hidden consequences of olfactory dysfunction: a patient report series. *BMC Ear Nose Throat Disord.* 23;13:8.
2. Kohli P, Soler ZM, Nguyen SA, Muus JS, Schlosser RJ. 2016 The Association Between Olfaction and Depression: A Systematic Review. *Chem Senses.* 41(6):479–86.
3. Spence C. 2015 Just how much of what we taste derives from the sense of smell? *Flavour.* 2;4(1):30.
4. Boesveldt S, Postma EM, Boak D, Welge-Luessen A, Schöpf V, Mainland JD, et al. 2017 Anosmia—A Clinical Review. *Chem Senses.* 42(7):513–23.
5. Menni C, Valdes AM, Freidin MB, Sudre CH, Nguyen LH, Drew DA, et al. 2020 Real-time tracking of self-reported symptoms to predict potential COVID-19. *Nat Med.* 26(7):1037–40.
6. Fullard ME, Morley JF, Duda JE. 2017 Olfactory Dysfunction as an Early Biomarker in Parkinson's Disease. *Neurosci Bull.* 33(5):515–25.
7. Noyce AJ, Lees AJ, Schrag A-E. 2016 The prediagnostic phase of Parkinson's disease. *J Neurol Neurosurg Psychiatry.* 87(8):871–8.
8. Charbonneau J, Relyea K. 1997 The technology behind on-page fragrance sampling. *Drug Cosmet Ind.* 160(2):48.
9. Doty RL, Shaman P, Dann M. 1984 Development of the University of Pennsylvania Smell Identification Test: a standardized microencapsulated test of olfactory function. *Physiol Behav.* 32(3):489–502.
10. Mariano FC, Hamerschmidt R, Soares CMC, Moreira AT. 2018 The Middle Turbinate Resection and Its Repercussion in Olfaction with the University of Pennsylvania Smell Identification Test (UPSIT). *Int Arch Otorhinolaryngol.* 22(3):280–3.
11. Morley JF, Cohen A, Silveira-Moriyama L, Lees AJ, Williams DR, Katzenschlager R, et al. 2018 Optimizing olfactory testing for the diagnosis of Parkinson's disease: item analysis of the university of Pennsylvania smell identification test. *NPJ Park Dis.* 4:2.
12. Auger SD, Kanavou S, Lawton M, Ben-Shlomo Y, Hu MT, Schrag AE, et al. 2020 Testing Shortened Versions of Smell Tests to Screen for Hyposmia in Parkinson's Disease. *Mov Disord Clin Pract.* 7(4):394–8.

13. Joseph, T., Auger, S. D., Peress, L., Rack, D., Cuzick, J., Giovannoni, G., Lees, A., Schrag, A. E., & Noyce, A. J. (2019). Screening performance of abbreviated versions of the UPSIT smell test. *Journal of neurology*, 266(8), 1897–1906.
14. Yanagida Y, editor A survey of olfactory displays: Making and delivering scents2012: IEEE.
15. Herrera NS, McMahan RP, editors. Development of a Simple and Low-Cost Olfactory Display for Immersive Media Experiences2014: ACM Press.
16. Martins E, Poncelet D, Rodrigues RC, Renard D. 2017 Oil encapsulation techniques using alginate as encapsulating agent: applications and drawbacks. *J Microencapsul*. 17;34(8):754–71.
17. A.S. Chaurasia, F. Jahanzad, S. Sajjadi. 2017 Preparation and characterization of tunable oil-encapsulated alginate microfibers. *Materials & Design*. 128, 64-70.
18. Yildirim E, Xu Q and Basaran O A 2005 Analysis of the drop weight method. *Phys. Fluids*. 17 062107.
19. Abang S, Chan ES, Poncelet D. 2012 Effects of process variables on the encapsulation of oil in Ca-alginate capsules using an inverse gelation technique. *J Microencapsul*, 29(5):417–28.
20. Kelly J. Cole , Diane L. Rotella, John G. Harper. 1999 Mechanisms for Age-Related Changes of Fingertip Forces during Precision Gripping and Lifting in Adults. *Journal of Neuroscience*. 19 (8) 3238-3247.